



Circulation anomalies in the Southern Hemisphere and ozone changes

P. Braesicke¹, J. Keeble², X. Yang¹, G. Stiller³, S. Kellmann³, N. L. Abraham¹, A. Archibald¹, P. Telford¹, and J. A. Pyle¹

¹NCAS/University of Cambridge, Chemistry Department, Cambridge, UK

²University of Cambridge, Chemistry Department, Cambridge, UK

³IMK-ASF, KIT, Karlsruhe, Germany

Correspondence to: P. Braesicke (pb261@cam.ac.uk)

Received: 30 January 2013 – Published in Atmos. Chem. Phys. Discuss.: 28 March 2013

Revised: 12 September 2013 – Accepted: 15 September 2013 – Published: 4 November 2013

Abstract. We report results from two pairs of chemistry-climate model simulations using the same climate model but different chemical perturbations. In each pair of experiments an ozone change was triggered by a simple change in the chemistry. One pair of model experiments looked at the impact of polar stratospheric clouds (PSCs) and the other pair at the impact of short-lived halogenated species on composition and circulation. The model response is complex with both positive and negative changes in ozone concentration, depending on location. These changes result from coupling between composition, temperature and circulation. Even though the causes of the modelled ozone changes are different, the high latitude Southern Hemisphere response in the lower stratosphere is similar. In both pairs of experiments the high-latitude circulation changes, as evidenced by N₂O differences, are suggesting a slightly longer-lasting/stronger stratospheric descent in runs with higher ozone destruction (a manifestation of a seasonal shift in the circulation). We contrast the idealised model behaviour with interannual variability in ozone and N₂O as observed by the MIPAS instrument on ENVISAT, highlighting similarities of the modelled climate equilibrium changes to the year 2006–2007 in observations. We conclude that the climate system can respond quite sensitively in its seasonal evolution to small chemical perturbations, that circulation adjustments seen in the model can occur in reality, and that coupled chemistry-climate models allow a better assessment of future ozone and climate change than recent CMIP-type models with prescribed ozone fields.

1 Introduction

The recent United Nations Environment Programme/World Meteorological Organization (UNEP/WMO) ozone assessment (WMO, 2011) highlights the importance of chemistry-climate interactions, emphasising the strong link between composition differences and climate change. For example, to first order, when the concentrations of halogen radical species decrease/increase in the stratosphere, we expect to see an increase/decrease in ozone. However, any ozone change will be coupled to changes in temperature and circulation, feeding back further onto the initial ozone change (e.g. low ozone in spring results in decreased short-wave heating rates); temperatures stay low for longer and the meridional temperature gradient remains steep; zonal winds increase and meridional transport of ozone and other trace gases is reduced. Changes in stratospheric temperature and circulation are also projected under increased greenhouse gas loading. Stratospheric temperatures will decline which, due to the temperature dependence of the controlling gas phase reactions, should lead to ozone increases away from polar latitudes. In addition, climate model simulations with increasing long-lived greenhouse gases consistently show a strengthening (e.g. enhanced tropical upwelling at 70 hPa) of the stratospheric overturning circulation, the so-called Brewer–Dobson circulation (BDC; after Brewer, 1949 and Dobson, 1956), which will affect the meridional distribution of ozone in the stratosphere. In consequence, modelled stratospheric age-of-air¹ decreases in the extratropical stratosphere

¹Age-of-air or, for short, age is a measure for the time it takes an air mass to travel from the troposphere to a particular point in the stratosphere (see, e.g. Waugh and Hall, 2002).

(Butchart et al., 2006). However, age-of-air trends estimated from trace gas observations at an inhomogeneous selection of locations (Engel et al., 2009) have not confirmed this model result. Recently, Bönisch et al. (2011) discussed the role of height varying trends in transit times (Birner and Bönisch, 2011), concluding that the shallow residual circulation branch shows a steady decrease in transit times from 1979 to 2009. Stiller et al. (2012) highlighted the inhomogeneous spatial behaviour of age-of-air trends derived from satellite observed SF₆. These could be possible reasons why Engel et al. (2009) in their spatially aggregated data set were unable to detect a trend. It also challenges modellers to better understand the causes of regional stratospheric circulation changes and age-of-air differences.

A number of studies have emphasised chemistry-climate interactions in the Southern Hemisphere (SH). There is clear evidence for the SH ozone hole having caused a change in the SH polar vortex dynamics (Thompson et al., 2011) and a shift in the tropospheric jets (Son et al., 2010). Furthermore, different levels of ozone depletion, in different models, tend to modify surface climate modes (e.g. Gillett and Thompson, 2003; Morgenstern et al., 2008), including the Southern and Northern Annual Modes. Changes in the stratospheric vortex/jet strength and position are also reflected in the overturning speed of the BDC.

Note that the BDC is not just one single overturning cell. It can be envisaged as a hemispheric to global scale circulation with three distinct height regimes as illustrated in Fig. 1, following Plumb (2002): a global scale branch with air flowing from the summer to the winter pole in the upper stratosphere and mesosphere (red), an upper/middle stratospheric branch with air flowing from the tropical region to middle and high latitudes in the winter hemisphere (orange), and a lower stratospheric/upper tropospheric branch flowing from tropical to middle and high latitudes in both hemispheres at all seasons, notwithstanding some seasonal modulation (green). All three branches are relevant to determining the composition and mean age of SH polar air in the lower stratosphere. We will investigate in idealised model experiments how a chemical change impacts the balance of the three BDC branches in the SH and, in turn, also affects composition. We will present evidence that such modulation of the BDC can be detected in observations.

We report results from two pairs of chemistry-climate model simulations using the same climate model with different chemistry schemes. Differences between the two runs in each pair of experiments show some commonalities regarding composition and circulation changes in the SH. We aim to characterise and explain the qualitatively similar changes and to put them into context with observed interannual variability. We do not provide a detailed analysis of the individual model runs (this is left to other publications in the near future from the co-authors Alex Archibald, James Keeble and Xin Yang). Here, we point out the common features in the differences between the two integrations in each of the

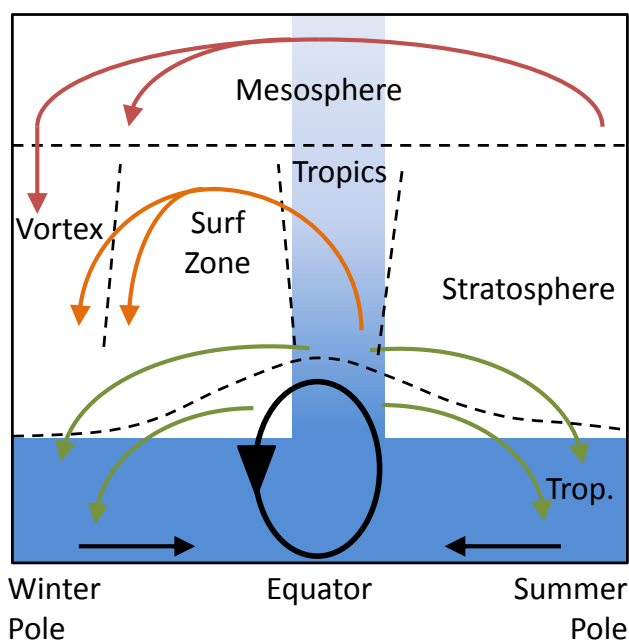


Fig. 1. Conceptual structure of the Brewer–Dobson circulation (BDC) following Plumb (2002). The three main circulation branches are highlighted in different colours, which are used in summary Fig. 12 to distinguish the height regions. Blue shadings indicate the general altitude gradient of N₂O with near-constant N₂O in the troposphere (Trop.). The complex meridional N₂O gradient structure in the stratosphere is shaped by the different BDC branches and is not detailed here.

two pairs of experiments that illustrate a robust chemistry-climate feedback between changes in ozone depletion and circulation differences.

We start by discussing details of our runs and the analysis strategy (Sect. 2), followed by the description of the modelled response (Sect. 3). Observational considerations and a case study supporting the model results are presented in Sect. 4. Section 5 summarises and presents a generalisation of the findings.

2 Method

The model is an update of the model described in Morgenstern et al. (2009). Compared to the model version contributing to the chemistry-climate model validation initiative phase 2 (CCMVal-2), the underlying Unified Model (UM) atmospheric climate model has been updated from version 6.1 to 7.3 (Hewitt et al., 2011). This improved the tropopause height and ozone bias in the model system. The integrations are performed with a horizontal resolution of 3.75° in longitude and 2.5° in latitude on an Arakawa-C grid. A hybrid sigma-geometric height coordinate is used to resolve the vertical range from the surface up to ~84 km with 60 levels, resulting in a vertical resolution of just above 1 km

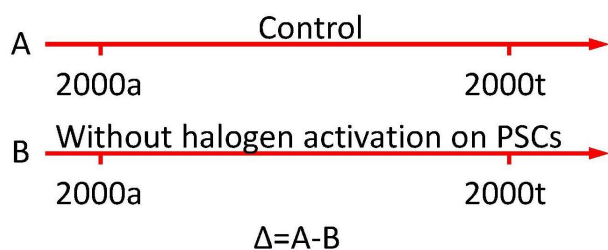
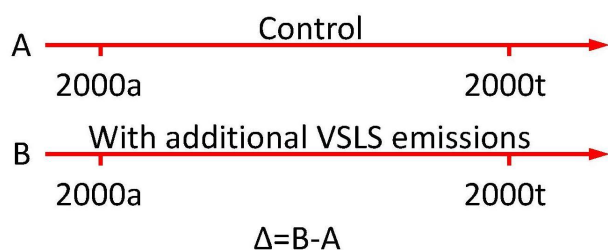
Pair A: UMUKCA CheS**Pair B: UMUKCA CheST+**

Fig. 2. Summary of the two pairs of experiments. Pair A compares integrations with and without halogen activation on PSCs. Pair B compares integrations with and without additional halogenated species emissions. The differences (Δ) are defined in a way that the run with generally higher ozone is subtracted from the run with lower ozone. See Fig. 3 for total ozone changes. Note that the runs are time slice integrations, and consecutive model years are for the same year 2000 boundary conditions. However, the individual years in each run differ due to internal variability as indicated by the letters behind all “2000” time-line labels.

in the lower stratosphere. All model integrations are performed for year 2000 boundary conditions. Averaged sea surface temperatures (SSTs) and sea ice concentrations (SICs) are prescribed. There is an annual cycle in the SST and SIC boundary conditions, but no interannual variability. The model can use a number of different chemistry schemes. Here a **Chemistry of the Stratosphere (CheS)** scheme based on Morgenstern et al. (2009), including some minor updates to reaction rates, is used within UM7.3 in experiment pair A. In experiment pair B the chemistry scheme includes a more detailed tropospheric volatile organic compound mechanism, and additional halogenated short-lived species and related reactions (CheST+; **Chemistry of the Stratosphere and Troposphere with additional halogenated short-lived species (+)**)². Both model set-ups use trace gases interactively in the calculation of heating rates allowing for feedbacks between changing circulation and composition.

²Effectively this scheme is an extended merger of CheS (see above) and the standard tropospheric chemistry CheT as described in O’Connor et al. (2009).

For each model set-up a pair of experiments is performed, as summarised in Fig. 2. One pair of model experiments (Pair A using the CheS model set-up) looks at the impact of PSCs. The second pair (Pair B using the CheST+ model set-up) considers the impact of short-lived halogenated species on composition and circulation. In the following we simply refer to pair A and pair B. Pair A consists of one model integration allowing chlorine activation on polar stratospheric clouds (PSCs) and one inhibiting the activation on PSCs. In this case, we expect a large impact in polar latitudes, with the integration that includes activation on PSCs leading to much lower ozone there. Pair B consists of one model integration where short-lived halogenated species are emitted in addition to the usual long-lived halogenated species and one not emitting these short-lived species. In this case we anticipate that the ozone differences will be largest in the very low stratosphere and have a more global extent than for pair A.

For each pair of integrations, differences are calculated by subtracting the run in which we expect higher ozone (lower ozone depletion) from the run with potentially higher ozone depletion, following the general rule of thumb, above, that a larger availability of halogenated species will lead to larger ozone destruction. This should lead to consistent signs in the model differences (Fig. 2). All runs are spun-up for 10 yr and are integrated for 20 (pair A) and 10 (pair B) years.

To characterise the changes in circulation and composition, including seasonality, we will consider model fields of zonal mean zonal wind (to discuss the polar vortex evolution and strength, and its impact on meridional transport), nitrous oxide (N_2O ; a tracer with a lifetime of around 120 yr, with its source in the troposphere; N_2O is suitable for assessing integrated seasonal transport changes and is well observed on a global scale by satellite instruments), ozone (O_3 ; lifetime of weeks to month in the lower stratosphere, with its major source in the stratosphere; O_3 is well observed and drives the modelled changes), mean age of air (an idealised tracer increasing linearly with time at the model surface, e.g. Waugh and Hall, 2002; mean age can be estimated on a global scale from SF_6 observations and indicates the effectiveness of meridional transport), tropopause height and temperature.

3 Model response

We start our discussion by looking at the changes in total ozone and zonal wind (Sect. 3.1). Subsequently we discuss the changes in tropopause height (Sect. 3.2), before detailing the zonal mean ozone and temperature changes in December (Sect. 3.3). Using high-latitude N_2O we will discuss changes in the large-scale circulation and support these conclusions by looking at the age-of-air differences for December (Sect. 3.4).

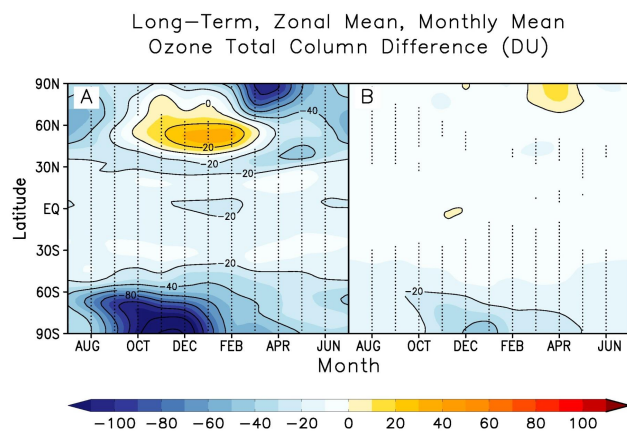


Fig. 3. Long-term, monthly and zonal mean total ozone differences (Dobson Units, DU) for experiment pairs A (left) and B (right). Negative differences are shown in cold colours and positive in warm colours. See Fig. 2 for definition of the differences. Differences that exceed one standard deviation of the “Control” are stippled.

3.1 Total ozone and zonal wind changes

Figure 3 shows the latitude-time evolution of zonal mean total ozone differences for the two experiment pairs A (left) and B (right). Stippled areas mark out regions where differences exceed one standard deviation of the run subtracted, thus indicating a likely significant change between runs in a pair. Even though it is important to know how significant modelled changes are, our arguments will focus on the consistency of composition and circulation changes and how they relate to each other during their seasonal development. Negative differences dominate in high southern latitudes in both experiment pairs. As expected Pair A, with PSCs switched on/off, and hence with the largest expected changes in activated chlorine, shows the larger negative change on the SH.

The response in the NH is quite complex, and in both cases some areas of ozone increase can be seen. Based simply on chemical arguments, for the one experiment with more reactive chlorine in each pair we would expect just to see an ozone decrease. The increases must be related to circulation changes, for example, possibly enhanced poleward transport during NH winter in pair A and an earlier vortex break-up in pair B, but the statistical significance of the modelled features is small.

In the SH the following picture emerges: the modelled timing of the maximum ozone deficit in the SH differs between the experiment pairs. The largest negative anomaly occurs in pair A between October and December, whereas the smaller negative anomaly in pair B occurs slightly later. In addition to the chemically induced ozone differences, dynamical changes also occur, as we will show below. For example, the lower stratospheric branch of the BDC acts as a year-round supply route for ozone from low to high latitudes. In contrast, the middle stratospheric branch of the BDC fulfils

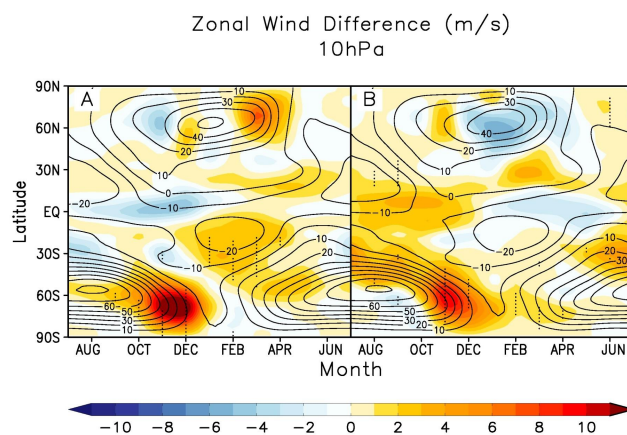


Fig. 4. Long-term, monthly and zonal mean zonal wind (isolines, m s^{-1}) and zonal wind differences (shadings, m s^{-1}) for experiment pairs A (left) and B (right) at 10 hPa. Positive differences are shown in warm colours and negative in cold colours. See Fig. 2 for definition of the differences. Differences that exceed one standard deviation of the “Control” are stippled.

this role most efficiently during winter (e.g. Grewe, 2006). As a consequence the relative effectiveness of these transport routes has a strong seasonality that plays a role in maintaining (or wiping out) high-latitude ozone anomalies from spring to summer, when the supply of ozone from the middle stratospheric branch of the BDC decays. Depending on the strength of the lower stratospheric BDC, the lifetime of the SH springtime “ozone mass deficit” (Bodeker et al., 2005) can either be enhanced or diminished. In our experiments the negative high-latitude SH ozone anomalies are long-lived from austral spring to summer, indicative of a weakened lower stratospheric BDC, similar to the pattern seen in Braesicke et al. (2006) for a doubling of CO_2 in a predecessor model. In addition, observational evidence from SF_6 derived age-of-air data supports this statement (Stiller et al., 2012), showing “old” polar air masses until late summer.

The ozone-based BDC interpretation above is supported by the changes of the zonal mean zonal winds in both pairs of integrations. Figure 4 shows the long-term monthly and zonal mean zonal wind at 10 hPa (isolines, m s^{-1}) and the zonal wind differences as defined in Fig. 2 (shaded, m s^{-1}). The climatological winds are in good agreement between pairs A and B. In the NH winds exceed 30 m s^{-1} from November onwards at 60°N and the stratospheric jet decays in March. In the SH winds exceed 30 m s^{-1} from March onwards at 60°S and the stratospheric jet decays in November/December. In both pairs a strengthening of the late stratospheric winter jet in the SH is modelled (this is similar to the negative stratospheric temperature trends diagnosed by Son et al. (2010) in the CCMVal-2 models during summer for the period 1960–1999). This also indicates a change in seasonality by a longer-lived vortex; the change is relatively coherent with height. In general terms a stronger vortex allows

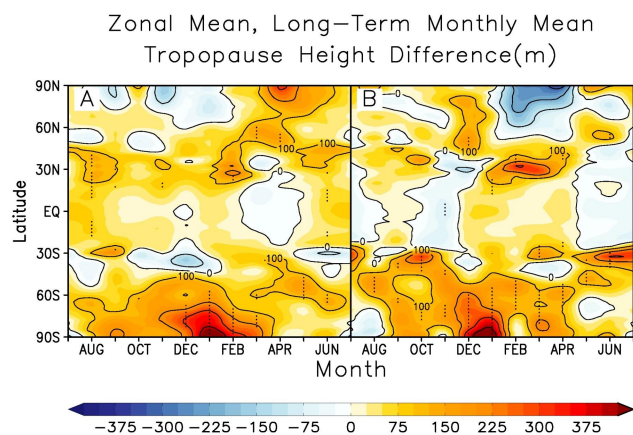


Fig. 5. Long-term, monthly and zonal mean WMO (lapse rate) tropopause height differences (metres) for experiment pairs A (left) and B (right). Positive differences are shown in warm colours and negative in cold colours. See Fig. 2 for definition of the differences. Differences that exceed one standard deviation of the “Control” are stippled.

less meridional transport, with a stronger more coherent circumpolar jet acting as a more efficient meridional transport barrier. This is consistent with a seasonally weakened BDC, as discussed above, and is illustrated by the negative polar ozone anomalies in the SH during late spring and early summer (Fig. 3) in conjunction with the positive wind anomalies in November (Fig. 4). Interestingly, even though the ozone changes modelled are different between the pairs of experiments, the relationship between stronger stratospheric winds and low ozone (or weaker stratospheric winds and high ozone respectively) holds in the NH as well. The relationship is physically consistent; the strength of the vortex, measured by the zonal wind, is a good indicator of effective meridional transport. This might not be too surprising, because the relationship also works well for interannual variations in winds and ozone in the stratosphere (Braesicke and Pyle, 2003), and should therefore also manifest itself in climatological means.

Given the proposed importance of circulation changes, we explore these further below. In subsequent subsections we will link the ozone changes to the modelled tropopause height changes and, then, more generally to BDC changes by discussing the changes in modelled N_2O distributions.

3.2 Tropopause height changes

Figure 5 shows the latitude-time evolution of zonal mean tropopause height differences for both experiment pairs. Positive differences dominate high SH latitudes, maximising in southern polar latitudes during austral summer when the ozone differences are also highest. Even though the SH responses are very similar in both experiment pairs, the Northern Hemisphere spring evolution differs between Pairs

A and B (note however that most NH changes are not statistically significant).

The total ozone differences shown in Fig. 3 are consistent with the tropopause behaviour seen in Fig. 5. Generally, a higher than average tropopause will result in lower than average column ozone in most latitudes. Dynamical control produces a shallower region of stratospheric ozone mixing ratios in the lowermost stratosphere above a high tropopause, leading to lower column ozone values when integrated vertically.

However, there are some differences in timing between ozone deficits (Fig. 3) and tropopause heights (Fig. 5). In pair A the largest ozone deficit precedes the period of highest tropopause; in pair B the largest ozone deficit occurs simultaneously with the highest tropopause. This difference is related to the more seasonal and regional change of ozone in A. Chemical ozone loss is suppressed in one integration by neglecting halogen activation on PSCs during Antarctic spring. The induced change in ozone leads to a different thermal structure (discussed in detail in the following section), including an elevated tropopause. As highlighted above a high tropopause is consistent with low column ozone, and thus a certain persistence of low column ozone episodes can be realised. Due to the strong chemical depletion in A the largest ozone deficit precedes the highest elevation of the tropopause. In experiment pair B the ozone change is more modest and stays in synchronisation with the tropopause change. Even though the initial “disturbance” to the system is the enhanced availability of reactive halogens which leads to increased ozone destruction, the dynamical signature as indicated by the high tropopause/low ozone during December/January in the SH is a dominant feature of the new equilibrium-climate state in both pairs of experiments.

To explore the common features during austral summer in more detail, we will next investigate the latitude-height structure of ozone and temperature changes for December.

3.3 Ozone and temperature changes in december

Figure 6 shows long-term monthly mean latitude-height cross sections of ozone differences for December, when peak column ozone differences occur in the Southern Hemisphere (Fig. 3). Pairs A and B both show a consistent decrease in lower stratospheric ozone in high southern latitudes in response to the changes implemented in each pair of model integrations.

As expected, in pair A the magnitude of ozone loss is larger in response to the suppression of halogen activation on PSCs. Pair B has the maximum loss slightly higher in altitude; in this case, halogen activation on PSCs is present in both runs but the abundance of reactive halogen is increased relative to A. In pair A the ozone difference south of 75° S and between 15 to 20 km exceeds 60%. In pair B only up to 30% difference is modelled in the Antarctic stratosphere. Even though the general expectation for the experiments is increased ozone loss, it should be noted that there are

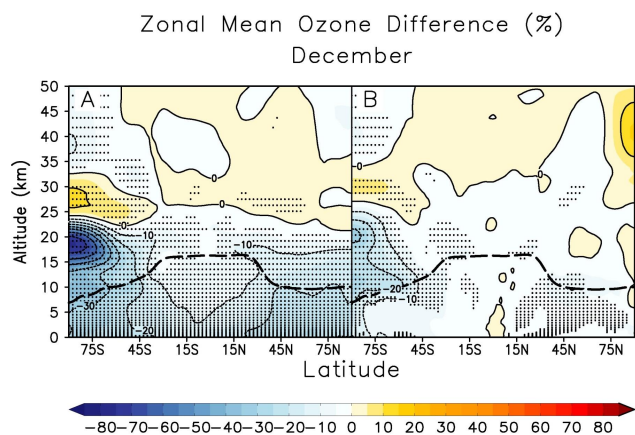


Fig. 6. December zonal and monthly mean ozone differences in percent (relative to the mean volume mixing ratio in the “Control” run) for experiment pair A (left) and experiment pair B (right). Negative differences are shown in cold colours and positive in warm colours. The black dashed line indicates the position of the tropopause in the base cases. Differences that exceed one standard deviation of the “Control” are stippled.

some areas in the mid- and upper stratosphere where ozone is slightly increased in response to complex composition–climate interaction for which it is difficult to disentangle cause and effect. The aggregated effect manifests itself in a seasonal shift of the BDC and we will summarise the changes in seasonality below.

The large tropospheric changes of ozone in pair A are in part due to the simple tropospheric chemistry in CheS, and also reflect changes in ozone exchange between the lowermost stratosphere and the uppermost troposphere (see for example Morgenstern et al. (2013) in which a 20 % increase of stratosphere–troposphere exchange for ozone recovery was diagnosed in UMUKCA); summer tropospheric ozone production does not mitigate the downward transport of a stratospheric ozone deficit. CheST+ (pair B) includes a comprehensive tropospheric chemistry and together with the smaller ozone changes in the lowermost stratosphere, tropospheric changes are also much smaller and less significant. The negative ozone anomalies in Fig. 6 are largely triggered by increased chemical ozone destruction, but they happen in conjunction with transport changes, in particular in high latitudes. Next we will discuss the simultaneous change in temperature during austral summer before discussing the integrated high-latitude circulation changes in the following section.

Figure 7 shows the temperature differences for experiment pairs A and B as a latitude–height cross section. Note that we focus our discussion here on SH early summer (December), when the high-latitude lower stratospheric ozone changes established in spring are still significant and will impact on the radiation in the model. In the SH the temperature response relates directly to the ozone differences shown in Fig. 6,

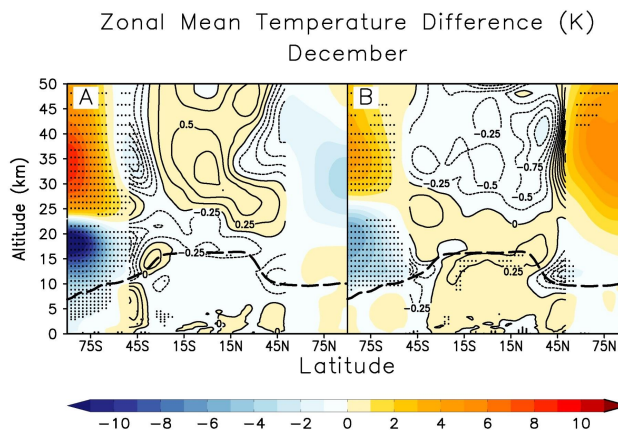


Fig. 7. December zonal and monthly mean temperature differences (K) for experiment pair A (left) and experiment pair B (right). Isolines are used to provide structural information for the much smaller tropical changes. Negative differences are shown in cold colours and positive in warm colours. The black dashed line indicates the position of the tropopause in the base cases. Differences that exceed one standard deviation of the “Control” are stippled.

with SH polar temperatures being lower where ozone is depleted (between 10 to 22 km) due to reduced short-wave heating rates. Above 25 km higher temperatures indicate largely a dynamical response with enhanced descent causing adiabatic warming. Due to feedbacks the situation is more complicated in lower latitudes. In some areas (e.g. the tropical stratosphere above 25 km in B), ozone increases where temperatures are lower, thus highlighting the slow-down of the gas-phase ozone loss reactions. In other areas signatures are far more complex. Contributing effects include: ozone differences above altering photolysis rates below, radiatively and dynamically induced temperature changes and their impact on chemistry, and transport changes. Quantifying the relative contributions of all effects is beyond the scope of this study.

For both model pairs the south polar responses are similar, with a larger magnitude in the case with a more severe ozone loss (pair A). The tropical and NH polar changes are very different between the two pairs of experiments and are not significant, due to high dynamical variability during NH winter. Despite the SH high-latitude similarities the tropical changes also differ between the pairs of experiments, with a negative temperature anomaly around and above the tropopause in pair A and a positive anomaly in pair B. This is also evident in the magnitude of the transport changes modelled in N_2O that are discussed in the next section.

3.4 Circulation changes

The use of tracer data to characterise transport changes is well established (e.g. Ray et al., 2002, 2010). Here we use N_2O to visualise changes in the modelled BDC. Figure 8 shows the seasonal progression of N_2O (isolines) and N_2O

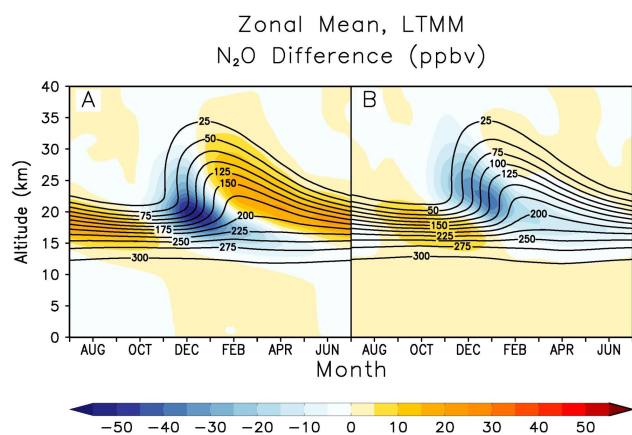


Fig. 8. Time-height cross sections of N_2O and N_2O differences. Isolines: absolute values of long-term monthly mean (LTMM) N_2O (parts per billion by volume, ppbv) averaged over all latitudes south of 70°S for runs subtracted in pair A (left) and pair B (right). Shadings: absolute differences in N_2O (ppbv) for experiment pair A (left) and experiment pair B (right). Positive differences are shown in warm colours and negative in cold colours.

differences (shaded) in high southern latitudes (averaged over all latitudes south of 70°S) from the surface to 40 km for both pairs of model integrations.

The absolute N_2O values (from the “high ozone” run that is subtracted in each pair of experiments) are shown as isolines; N_2O differences between runs in each experiment pair are shaded. Starting in SH late summer (February), the downward slope of the isolines is indicative of the high-latitude descending branch of the Brewer–Dobson circulation. This compares well to the seasonal development of the residual stream functions shown in Fig. 3 of Seviour et al. (2012) and the rapid strengthening of the high-latitude downwelling between December, January, February and March, April, May means. Following Plumb (2002) and as indicated in Fig. 1, during autumn and winter the two upper vertical regions of the BDC contribute to the pronounced descent visualised by the downward slope of the N_2O isolines. During spring a strong vertical gradient in N_2O is maintained. Note how rapidly N_2O increases again in early summer (November/December) above 25 km when the upper part of the BDC undergoes significant seasonal change (Seviour et al., 2012).

Positive anomalies in autumn (persisting until winter) indicate stronger meridional transport and decreased descent in the “low ozone” run, which can be interpreted as a strengthening of the meridional drift of the middle BDC branch bringing more N_2O to high latitudes and a weakening of the uppermost descending BDC branch, which would otherwise bring low N_2O down. Subsequently, the negative anomalies below 25 km during spring/summer indicate an enhanced/prolonged descent bringing low N_2O down in altitude over a longer period during which ozone concentrations are decreased. In addition, a weaker middle/lower

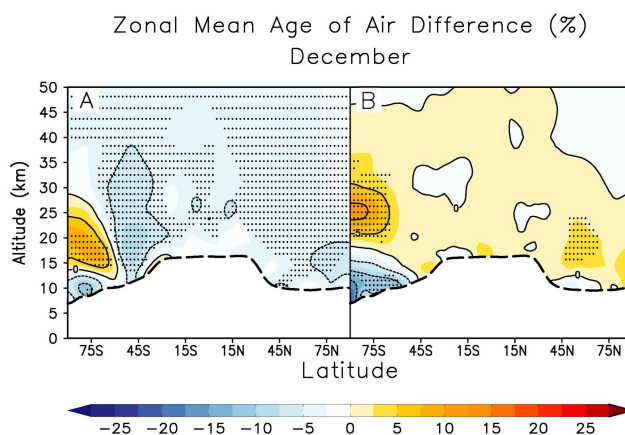


Fig. 9. December zonal and monthly mean age-of-air differences in percent for experiment pair A (left) and experiment pair B (right). Positive differences are shown in warm colours and negative in cold colours. The black dashed line indicates the position of the tropopause in the “Control” cases. Differences that exceed one standard deviation of the “Control” are stippled.

stratospheric BDC branch does not replenish high-latitude N_2O as effectively from the tropical entry point. This agrees well with the positive high-latitude anomalies in zonal mean zonal winds lasting from October to January (Fig. 4 and discussion above), and the associated change in seasonality of the BDC that is linked to the stratospheric vortex lifetime. The vortex lasts 15 to 20 days longer in integrations with more severely depleted ozone (more details are discussed below).

Positive N_2O anomalies around 15 km indicate a strengthening of the lowermost stratospheric BDC branch and at 25 km a strengthening of the middle stratospheric BDC branch, an assertion that is verified by the (not directly observable) transformed Eulerian mean circulation diagnostics (Andrews et al., 1987) available from pair A (not shown), in which the poleward residual meridional velocities are generally enhanced. In contrast, positive N_2O anomalies just above the Antarctic tropopause result from enhanced mixing with tropospheric air in conjunction with the elevation of the tropopause.

Figure 9 shows latitude-height cross sections of relative mean age-of-air differences above the tropopause for each pair of experiments during December. For both pairs, the mean age-of-air difference shows a dipole structure in high southern latitudes with younger air just above the tropopause and older air around or slightly above 15 km. This pattern suggests more efficient mixing slantwise across and along the elevated tropopause in high latitudes (younger air anomaly, blue) and a weakened lower to middle stratospheric BDC branch, advecting less young air from lower latitudes (older air anomaly, orange). This is consistent with the longer-lived SH polar vortex in runs with more ozone depletion, because a more pronounced vortex edge suppresses meridional

transport. In both pairs of experiments the general structure of the high latitude SH pattern is similar. The amplitude of the feature is slightly larger in pair B, where we expect a more year-round global change of chemistry, compared to the more regional and seasonal change in pair A (the PSC experiments). The larger vertical extent of the area of younger air above the Antarctic tropopause in B is consistent with the longer duration of a positive anomaly in N_2O (Fig. 8), both indicating a more effective exchange of air between the upper troposphere and the lowermost stratosphere during December in B as compared to A, where the positive N_2O anomaly starts earlier and does not last throughout December.

Changes in age equatorward of 60° S differ between experiment pairs A and B. In A age is generally decreased whereas in B age is generally higher (B being the experiment pair with less seasonality). Note that the change in A is nearly everywhere significant (stippled area, as defined in Sect. 3.1), whereas the change in B is only significant in high southern latitudes and, to some degree, in northern middle latitudes. Note, also, that the differences in age-of-air between pairs A and B away from the SH polar region are consistent with the modelled changes in zonal mean temperature, with younger air (blue) in A where lower temperatures at the tropopause indicate a strengthened upwelling and older air (yellow) in B where higher temperatures at the tropopause indicate a weakened upwelling (Fig. 7). The ozone change is more complex, because it depends on a coupled chemistry-transport response. In A the tropical lower stratospheric decrease in ozone is consistent with the increased uplift. In both experiment pairs the ozone changes in the upper stratosphere are anti-correlated with the temperature changes, as expected for ozone in photochemical steady state. In B, the decrease in ozone in the tropical lower stratosphere is driven by the change in available bromine from the short-lived halogenated species that occurs at all latitudes and during all months.

In summary, the changes in ozone and circulation are intimately linked with temperature and tropopause height differences, with a higher tropopause indicating a stronger tropospheric influence on the lowermost stratosphere and hence younger air. Interpreting our results it is important to appreciate the more seasonal and regional trigger in A in contrast to the year-round, global trigger in B. By definition the changes in each pair are different, but they are embedded in the naturally occurring seasonal cycle. Despite many differences, some of the impact manifests itself in similar changes in hemispheric transport patterns, especially near the South Pole. The similarities in SH N_2O anomalies (Fig. 8) between A and B are indicative of similar changes in the seasonal progression of the BDC, and in the summer change in age-of-air (Fig. 9) that is linked to an elevated SH high-latitude tropopause. This links directly to the evidence chain presented in conjunction with Fig. 3 (above), relating the lifetime of a SH polar ozone mass deficit to the strength of the BDC.

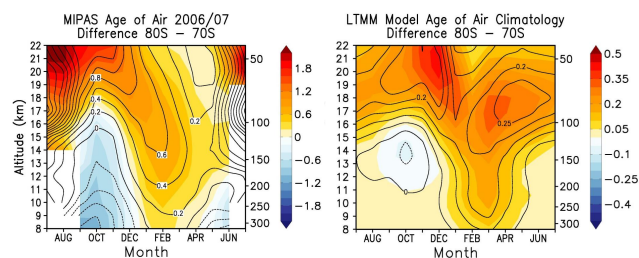


Fig. 10. MIPAS observed (left) and UMUKCA modelled (right) time-height cross sections of age-of-air differences between 80° S and 70° S. For MIPAS the year 2006–2007 is shown in isolines and the climatology is shaded. For UMUKCA pair A is shown (shaded: experiment with PSCs; isolines: experiment without PSCs). The scales for age gradients are different to highlight the patterns (e.g. sign reversal). Note that the meridional gradient is stronger for the MIPAS observed case: for MIPAS the orange shading indicates an age difference above 0.6 yr, for the model the same colour indicates an age difference around 0.2 yr. Positive differences are shown in warm colours and negative in cold colours.

4 MIPAS observations

For nearly a decade (2002–2012) the Michelson Interferometer for Passive Atmospheric Sounding (MIPAS) instrument on ENVISAT (“Environmental Satellite”) has successfully observed atmospheric trace gas distributions. Here we use SF_6 derived age-of-air (Stiller et al., 2012) to validate the seasonality of the modelled high-latitude circulation. The subsequent case study for 2006–2007 uses a recent version (V5R_x_220) of MIPAS N_2O and ozone data processed at “Institut für Meteorologie und Klimaforschung/Instituto de Astrofísica de Andalucía” (IMK/IAA, updated from von Clarmann et al., 2009) to highlight interannual circulation changes and accompanying ozone differences.

4.1 Seasonality

As a way of validation of the modelled seasonal progression of the BDC we discuss the observed and modelled high-latitude age-of-air gradients. Figure 10 shows the seasonal progression of age-of-air differences between 80° S and 70° S (from the edge region (70° S), where large changes are modelled, towards the inner vortex (80° S) during winter) as a function of height for the observations (left) and experiment pair A (right). In observations, air at 70° S is older than air at 80° S below 16 km during spring. This is presumably related to horizontal mixing processes below the vortex linked to meridional drift in the lowermost stratospheric branch of the BDC and the different descent rates between the vortex core and a vortex region more towards the edge.

Above 16 km, air deeper inside the vortex is older compared to air more outside the vortex. The resulting strong gradient during late winter/early spring is artificially enhanced in the observations (Fig. 10, left) due to very old mean age

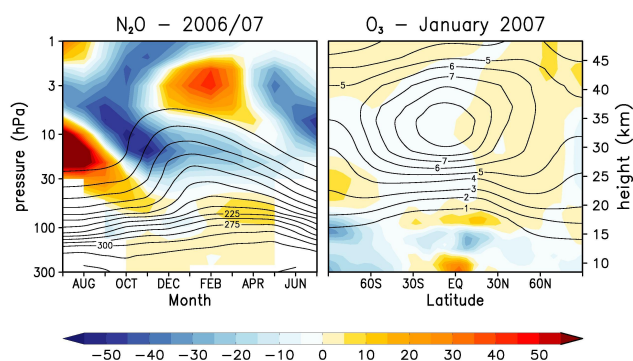


Fig. 11. Time–pressure cross section of climatological MIPAS N₂O (ppbv, isolines, left) and N₂O differences between 2006–2007 and the climatology (ppbv, shaded, left), both averaged over all latitudes south of 70° S. Latitude–pressure cross section of climatological January MIPAS ozone (ppmv, isolines, right) and ozone differences between January 2007 and the climatology (ppbv, shaded, right). Positive differences are shown in warm colours and negative in cold colours.

estimates in the vortex, caused by mesospheric SF₆ loss that cannot fully be accounted for in the derivation of the observed mean age. This structure is not seen in the model (Fig. 10, right), and the gradient reversal at lower altitudes is less pronounced. The signature of older air in higher latitudes becomes more prominent at lower altitudes during summer in both observations and model. The seasonality of the age gradient is a robust feature of the atmospheric circulation; neither in the observed case study or climatology (left, isolines and shadings) nor in the climatological means of both experiments in pair A (right, shadings and isolines) is the overall seasonality very different. Nevertheless, small changes can occur on top of the overall mean seasonality and are observed and modelled. We will discuss next these small changes, merging the ozone, N₂O and circulation differences into a consistent framework, diagnosing a change in the seasonality of the BDC.

4.2 Case study for 2006–2007

Isolines in Fig. 11 (left) show the climatological mean of N₂O from MIPAS observations for the period 2005–2012 using all months where data is available. The structural agreement between the observed and modelled climatological N₂O is high (see Fig. 8), indicating that the model captures the seasonal changes in high-latitude circulation well, as is also indicated by the age-of-air gradient shown in Fig. 10. Screening all annual N₂O anomalies, we find a particular year (2006–2007; shadings in Fig. 11, left) that shows clear similarities with the transport change patterns identified in our idealised model studies, in particular the descending negative anomaly from September to February (Fig. 8). In addition, the ozone change observed for January 2007 (shaded in

Fig. 11, right) shows a similar pattern to the modelled structure (c.f. the SH polar dipole in Fig. 6 between 12 and 32 km).

This good correspondence between N₂O differences modelled (Fig. 8) and observed during a particular year (Fig. 9) provides us with some confidence that the modelled seasonal BDC change could be relevant for the real atmosphere. In other words: the climatological change modelled can be seen in observed interannual variability. No causal relationship between ozone and N₂O anomalies can be implied from the observations. Nevertheless the model results would imply that halogen changes and their effects on ozone in the atmosphere could cause a seasonal shift in the circulation, towards a state of the atmosphere more similar to the SH condition of 2006–2007.

As mentioned before, we are not concluding that the change seen in the observations originates from the same initial disturbance we imprint on the model (e.g. the ozone difference in January 2006 was different). We compare modelled differences for climate equilibrium states (e.g. Fig. 8a and b), with a particular event in the real atmosphere. However, the similarity between the modelled and observed anomalies seems to indicate that our model results can be realised in the “real world”. As pointed out by Salby et al. (2012), both the change in stratospheric ozone and circulation in a particular month may have the same cause, and we just observe/model a consistent response of the system.

5 Summary and conclusions

We report results from two pairs of chemistry–climate model simulations using the same climate model but different chemistries. In each pair of experiments an ozone change was triggered by a simple change in the chemistry. One pair of model experiments looked at the impact of PSCs and the other at the impact of short-lived halogenated species on composition and circulation. In both pairs of experiments, although the run with higher active chlorine has less ozone globally, there are regions of the atmosphere, and particular periods, where ozone is increased locally. The response to the perturbations is not purely chemical but is an example of a chemical–dynamical–radiative feedback (or chemistry–climate feedback). In tropical and northern latitudes, the model responses differ between pairs A and B, although the temperature and ozone changes are consistent within each pair and reduced column ozone is consistently associated with an increased tropopause height. In the SH, the two pairs of experiments have a consistent response. In both pairs of integrations the Antarctic polar ozone destruction is increased due to the higher availability of reactive chlorine (and bromine) in one of the integrations. Even though the magnitude of the chemical change differs between experiments, a common response pattern in circulation could be detected. We now focus our discussion on this region.

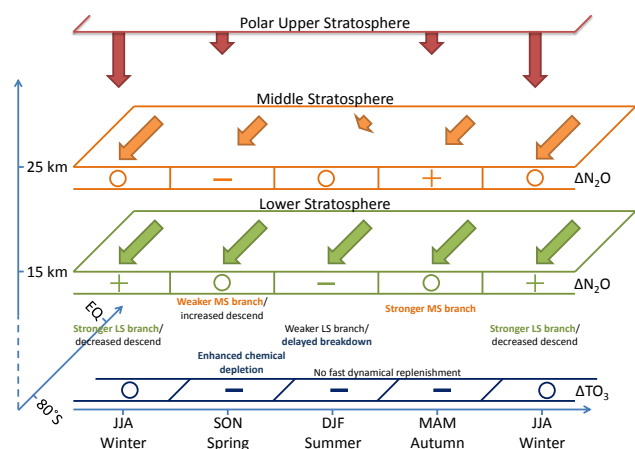


Fig. 12. Sketch summarising the time evolution of the changes modelled (LS: lower stratospheric, MS: middle stratospheric). Arrows indicate a mean state. Deviations are indicated with + (positive), – (negative) and o (neutral).

5.1 Schematic summary of model results

A schematic of the robust results emerging from experiment pairs A and B is shown in Fig. 12. The x axis represents the seasonal progression of the year, the y axis indicates latitude with high southern latitudes being to the front, and the z axis indicates altitude regions with around 15 km and 25 km highlighted. The +, – and o symbols indicate positive, negative and neutral anomalies between runs within a pair of integrations (pair A or B). ΔTO_3 is the difference in total ozone, and ΔN_2O is the difference in nitrous oxide mixing ratio. The arrows indicate the general seasonal cycle of the BDC found in each run, colour coded as in Fig. 1. Green arrows show the mean meridional drift of the lower stratospheric BDC branch, orange arrows indicate the mean seasonal evolution of the middle stratospheric BDC branch. Red arrows indicate descent due to the polar convergence of the uppermost branch of the BDC.

Within each pair of experiments, the fundamental, consistent difference is that in the run with the increased amount of active halogen, the SH spring ozone depletion is more severe (negative ΔTO_3). This negative anomaly carries through to summer and maximises around December, because of a delayed vortex breakdown in integrations with larger amounts of ozone depleted in spring. In addition the lower stratospheric branch of the BDC is slightly weakened (negative ΔN_2O around 15 km), thus inhibiting an efficient replenishment of ozone from the tropical lower stratospheric ozone production region. Consequently the negative total ozone anomaly is very long lived and persists into autumn.

In autumn the middle stratospheric branch of the BDC strengthens in the runs with higher ozone depletion (positive ΔN_2O around 25 km). This is followed by a positive N_2O anomaly lower down in winter, which occurs because the

positive anomaly from the previous season is advected downwards with the onset of descent linked to the uppermost BDC branch and is maintained by a strengthening of the lower stratospheric BDC branch (also evidenced by increased mid-latitude meridional heat flux at 150 hPa from June to August; not shown), which increases ozone transport from low to high latitudes as well.

The positive N_2O anomaly is maintained throughout winter by the strengthened lower stratospheric branch and a decrease in descent rates. Consistently, in the following spring seasonal negative N_2O anomalies around 25 km indicate a weakening (related to a later onset) of the middle stratospheric branch of the BDC (the September meridional heat flux anomaly in middle latitudes is negative; not shown) and slightly increased descent from above. This starts the seasonal cycle of changes again: in conjunction with the increased ozone depletion in spring this leads to a delayed break-up of the polar vortex during December.

As a caveat it should be mentioned that the Antarctic vortex in all model integrations presented here is slightly longer lived than observations would suggest. In many reanalyses data sets (see e.g. Fig. 4.2 of the CCMVal-2 Report, <http://www.sparc-climate.org/publications/sparc-reports/sparc-report-no5/>), the transition to easterlies at 60° S and 10 hPa occurs in late November. The previous model version (labelled UMUKCA-UCAM in the CCMVal-2 Report) captured this timing very well. In the integrations here the earliest break-up is modelled without halogen activation on PSCs using the CheS chemistry and occurs in early December. With halogen activation on PSCs the break-up is delayed by ~ 20 days (at 10 hPa, experiment pair A). The more comprehensive CheST+ chemistry (which always includes halogen activation by PSCs) has its transition in between the two dates for experiment pair A, and including additional halogen-containing compounds increases the ozone deficit and delays the break-up by ~ 18 days (at 10 hPa, experiment pair B).

5.2 Implications of the results

Much of what we describe does not allow for inference of causality; it merely points to a consistent change of the seasonal BDC development in both model integrations with enhanced ozone depletion in Antarctic spring. The delay of the vortex break-up in response to enhanced polar ozone depletion has been described before (e.g. Langematz et al., 2003), and is one of the important drivers of the change during other seasons. Certainly other aspects are also changing: planetary wave propagation in conjunction with the delayed vortex break-up (at 60° S meridional heat transport anomalies are negative during September to November; not shown), but in addition because generally ozone and thermal gradients have changed.

What we have presented here is a robust chemistry-climate feedback – one of many that require further investigation.

Many Intergovernmental Panel on Climate Change (IPCC)-type climate models do not have interactive ozone and so do not allow readjustments of stratospheric ozone and circulation (see the discussion in Son et al., 2010). If we would like to predict future climate change reliably and with narrowing uncertainties, our results suggest that we need to understand more about fairly small composition changes that can contribute to systematic changes in the hemispheric circulation. chemistry-climate models with detailed stratospheric chemistry are an important tool in the research armoury. As always there is a caveat regarding the general applicability of our results as all models exhibit some bias with respect to observations. Nevertheless, we are able to identify similar consistent changes in MIPAS data of the recent past as part of the interannual variability of the stratospheric climate system. So we believe that a future change in composition could lead to a systematic shift in the mean seasonal cycle of the BDC in the long term, beyond the general strengthening postulated for increasing long-lived greenhouse gases.

Feedbacks between composition and circulation are important in shaping our future climate. The above is just one particular example in which an initial composition change (increased availability of halogens) leads to a readjustment of the equilibrium state of the coupled chemistry-climate system. The overall ozone changes are determined by the initial composition change and the readjusted circulation (because the ozone change has changed heating rates and in conjunction winds). Understanding these processes in models and observations will lead to improvements in our ability to model the past climate and to project future changes more reliably.

Acknowledgements. We thank NCAS-CMS for modelling support. Model integrations have been performed using the UK National Supercomputing Service HECToR. P. Braesicke and J. Keeble thank NERC for support through grant NE/H024778/1. J. A. Pyle and X. Yang thank ERC for support through the ACCI grant and the EU for support through SHIVA. We thank two anonymous reviewers for their constructive criticism that helped us to improve aspects of the paper.

Edited by: W. Lahoz

References

- Andrews, D. G., Holton, J. R., and Leovy, C. B.: *Middle Atmosphere Dynamics*, Academic Press, 1987.
- Birner, T. and Bönisch, H.: Residual circulation trajectories and transit times into the extratropical lowermost stratosphere, *Atmos. Chem. Phys.*, 11, 817–827, doi:10.5194/acp-11-817-2011, 2011.
- Bodeker, G. E., Shiona, H., and Eskes, H.: Indicators of Antarctic ozone depletion, *Atmos. Chem. Phys.*, 5, 2603–2615, doi:10.5194/acp-5-2603-2005, 2005.
- Bönisch, H., Engel, A., Birner, Th., Hoor, P., Tarasick, D. W., and Ray, E. A.: On the structural changes in the Brewer–Dobson circulation after 2000, *Atmos. Chem. Phys.*, 11, 3937–3948, doi:10.5194/acp-11-3937-2011, 2011.
- Braesicke, P. and Pyle, J. A.: Changing ozone and changing circulation in northern mid-latitudes: Possible feedbacks?, *Geophys. Res. Lett.*, 30, 1059 doi:10.1029/2002GL015973, 2003.
- Braesicke, P., Hurwitz, M. M., and Pyle, J. A.: The stratospheric response to changes in ozone and carbon dioxide as modelled with a GCM including parameterised ozone chemistry, *Meteorol. Z.*, 15, 343–354, doi:10.1127/0941-2948/2006/0124, 2006.
- Brewer, A. W.: Evidence for a world circulation provided by the measurements of helium and water vapour distribution in the stratosphere, *Q. J. Roy. Meteor. Soc.*, 75, 351–363, 1949.
- Butchart, N., Scaife, A. A., Bourqui, M., de Grandpre, J., Hare, S. H. E., Kettleborough, J., Langematz, U., Manzini, E., Sassi, F., Shibata, K., Shindell, D., and Sigmond, M.: Simulations of anthropogenic change in the strength of the Brewer–Dobson, circulation, *Clim. Dynam.*, 27, 727–741, doi:10.1007/s00382-006-0162-4, 2006.
- CCMVal-2 Report: SPARC Report on the Evaluation of Chemistry–Climate Models, WCRP-132, WMO/TD No. 1526, SPARC Report No. 5, 2010.
- Dobson, G. M. B.: Origin and distribution of the polyatomic molecules in the atmosphere, *P. R. Soc. London*, A236, 187–193, 1956.
- Engel, A., Moebius, T., Boenisch, H., Schmidt, U., Heinz, R., Levin, I., Atlas, E., Aoki, S., Nakazawa, T., Sugawara, S., Moore, F., Hurst, D., Elkins, J., Schauffler, S., Andrews, A., and Boering, K.: Age of stratospheric air unchanged within uncertainties over the past 30 years, *Nat. Geosci.*, 2, 28–31, doi:10.1038/NGEO388, 2009.
- Gillett, N. P. and Thompson, D. W. J.: Simulation of recent Southern Hemisphere climate change, *Science*, 302, 273–275, doi:10.1126/science.1087440, 2003.
- Grewe, V.: The origin of ozone, *Atmos. Chem. Phys.*, 6, 1495–1511, doi:10.5194/acp-6-1495-2006, 2006.
- Hewitt, H. T., Copsey, D., Culverwell, I. D., Harris, C. M., Hill, R. S. R., Keen, A. B., McLaren, A. J., and Hunke, E. C.: Design and implementation of the infrastructure of HadGEM3: the next-generation Met Office climate modelling system, *Geosci. Model Dev.*, 4, 223–253, doi:10.5194/gmd-4-223-2011, 2011.
- Langematz, U., Kunze, M., Krüger, K., Labitzke, K., and Roff, G. L.: Thermal and dynamical changes of the stratosphere since 1979 and their link to ozone and CO₂ changes, *J. Geophys. Res.*, 108, 4027, doi:10.1029/2002JD002069, 2003.
- Morgenstern, O., Braesicke, P., Hurwitz, M. M., O’Connor, F. M., Bushell, A. C., Johnson, C. E., and Pyle, J. A.: The World Avoided by the Montreal Protocol, *Geophys. Res. Lett.*, 35, L16811, doi:10.1029/2008GL034590, 2008.
- Morgenstern, O., Braesicke, P., O’Connor, F. M., Bushell, A. C., Johnson, C. E., Osprey, S. M., and Pyle, J. A.: Evaluation of the new UKCA climate-composition model – Part 1: The stratosphere, *Geosci. Model Dev.*, 2, 43–57, doi:10.5194/gmd-2-43-2009, 2009.
- Morgenstern, O., Zeng, G., Abraham, N. L., Telford, P. J., Braesicke, P., Pyle, J. A., Hardiman, S. C., O’Connor, F. M., and Johnson, C. E.: Impacts of climate change, ozone recovery, and increasing methane on surface ozone and the tropospheric

- oxidizing capacity, *J. Geophys. Res.-Atmos.*, 118, 1028–1041, doi:10.1029/2012JD018382, 2013.
- O'Connor, F. M., Johnson, C. E., Morgenstern, O., and Collins, W. J.: Interactions between tropospheric chemistry and climate model temperature and humidity biases, *Geophys. Res. Lett.*, 36, L16801, doi:10.1029/2009GL039152, 2009.
- Plumb, R. A.: Stratospheric transport, *J. Meteorol. Soc. JPN*, 80, 793–809, doi:10.2151/jmsj.80.793, 2002.
- Ray, E. A., Moore, F. L., Elkins, J. W., Hurst, D. F., Romashkin, P. A., Dutton, G. S., and Fahey, D. W.: Descent and mixing in the 1999–2000 northern polar vortex inferred from in situ tracer measurements, *J. Geophys. Res.-Atmos.*, 107, 8285, doi:10.1029/2001JD000961, 2002.
- Ray, E. A., Moore, F. L., Rosenlof, K. H., Davis, S. M., Boenisch, H., Morgenstern, O., Smale, D., Rozanov, E., Hegglin, M., Pitari, G., Mancini, E., Braesicke, P., Butchart, N., Hardiman, S., Li, F., Shibata, K., and Plummer, D. A.: Evidence for changes in stratospheric transport and mixing over the past three decades based on multiple data sets and tropical leaky pipe analysis, *J. Geophys. Res.-Atmos.*, 115, D21304, doi:10.1029/2010JD014206, 2010.
- Salby, M. L., Titova, E. A., and Deschamps, L.: Changes of the Arctic ozone hole: Controlling mechanisms, seasonal predictability, and evolution, *J. Geophys. Res.-Atmos.*, 117, D10111, doi:10.1029/2011JD016285, 2012.
- Seviour, W. J. M., Butchart, N., and Hardiman, S. C.: The Brewer-Dobson circulation inferred from ERA-Interim, *Q. J. Roy. Meteor. Soc.*, 138, 878–888, doi:10.1002/qj.966, 2012.
- Son, S.-W., Gerber, E. P., Perlwitz, J., Polvani, L. M., Gillett, N. P., Seo, K.-H., Eyring, V., Shepherd, T. G., Waugh, D., Akiyoshi, H., Austin, J., Baumgaertner, A., Bekki, S., Braesicke, P., Bruehl, C., Butchart, N., Chipperfield, M. P., Cugnet, D., Dameris, M., Dhomse, S., Frith, S., Garny, H., Garcia, R., Hardiman, S. C., Joeckel, P., Lamarque, J. F., Mancini, E., Marchand, M., Michou, M., Nakamura, T., Morgenstern, O., Pitari, G., Plummer, D. A., Pyle, J., Rozanov, E., Scinocca, J. F., Shibata, K., Smale, D., Teyssedre, H., Tian, W., and Yamashita, Y.: Impact of stratospheric ozone on Southern Hemisphere circulation change: A multimodel assessment, *J. Geophys. Res.-Atmos.*, 115, D00M07 doi:10.1029/2010JD014271, 2010.
- Stiller, G. P., von Clarmann, T., Haenel, F., Funke, B., Glatthor, N., Grabowski, U., Kellmann, S., Kiefer, M., Linden, A., Losow, S., and López-Puertas, M.: Observed temporal evolution of global mean age of stratospheric air for the 2002 to 2010 period, *Atmos. Chem. Phys.*, 12, 3311–3331, doi:10.5194/acp-12-3311-2012, 2012.
- Thompson, D. W. J., Solomon, S., Kushner, P. J., England, M. H., Grise, K. M., and Karoly, D. J.: Signatures of the Antarctic ozone hole in Southern Hemisphere surface climate change, *Nat. Geosci.*, 4, 741–749, doi:10.1038/NGEO1296, 2011.
- von Clarmann, T., Höpfner, M., Kellmann, S., Linden, A., Chauhan, S., Funke, B., Grabowski, U., Glatthor, N., Kiefer, M., Schieferdecker, T., Stiller, G. P., and Versick, S.: Retrieval of temperature, H₂O, O₃, HNO₃, CH₄, N₂O, ClONO₂ and ClO from MIPAS reduced resolution nominal mode limb emission measurements, *Atmos. Meas. Tech.*, 2, 159–175, doi:10.5194/amt-2-159-2009, 2009.
- Waugh, D. W. and Hall, T. M.: Age of stratospheric air: Theory, observations, and models, *Reviews of Geophysics*, 40, 1010, doi:10.1029/2000RG000101, 2002.
- WMO, 2011: World Meteorological Organization Global Ozone Research and Monitoring Project – Report No. 52, Scientific Assessment of Ozone Depletion: 2010, 2011.